Mechanical Properties of Lipid Bilayers: A Note on the Poisson Ratio

M. Mert Terzi,[1, a)] Markus Deserno,[1, b)] and John F. Nagle[1, c)]
[1] *Department of Physics, Carnegie Mellon University, Pittsburgh, PA 15213, USA*

(Dated: 26 July 2020)

We investigate the Poisson ratio ν of fluid lipid bilayers, *i. e.*, the question how area strains compare to the changes in membrane thickness (or, equivalently, volume) that accompany them. We first examine existing experimental results on the area- and volume compressibility of lipid membranes. Analyzing them within the framework of linear elasticity theory for homogeneous thin fluid sheets leads us to conclude that lipid membrane deformations are to a very good approximation volume-preserving, with a Poisson ratio that is likely about 3% smaller than the common soft matter limit $\nu = \frac{1}{2}$. These results are fully consistent with atomistic simulations of a DOPC membrane at varying amount of applied lateral stress, for which we instead deduce ν by directly comparing area- and volume strains. To assess the problematic assumption of transverse homogeneity, we also define a depth-resolved Poisson ratio $\nu(z)$ and determine it through a refined analysis of the same set of simulations. We find that throughout the membrane's thickness, $\nu(z)$ is close to the value derived assuming homogeneity, with only minor variations of borderline statistical significance.

Keywords: lipid membrane, elasticity, Poisson ratio, simulation

I. INTRODUCTION

Biomembranes and lipid bilayers exhibit many interesting mechanical properties. Much emphasis has been placed on the bending modulus K_C, which is important for describing the flexural rigidity of membranes, and the area modulus K_A, which pertains to in-plane compression or stretching. These two are in fact conceptually related, but the details depend on additional microscopic assumptions, leaving the precise connection open to debate.[1–5] Since local surface geometry is described by two independent curvatures, the bending modulus K_C, which penalizes mean curvature, has a partner K_G, which quantifies the cost of Gaussian curvature. However, due to the Gauss-Bonnet theorem the Gaussian modulus usually only matters when the topology changes (say, pore opening or fission/fusion events), and for the same reason it is also very difficult to measure.[6–10]

A mechanical property of lipid membranes that has seen considerably less attention is their Poisson ratio, ν. This is the quantity that allows us to address the question: what relative area change $\Delta A/A$ results if we impose a relative thickness change $\Delta D/D$? Within linear elasticity, the ratio between these two quantities, multiplied by $-\frac{1}{2}$, is called the Poisson ratio.

It is frequently assumed in biophysics, often without noting it explicitly, that volume remains constant upon membrane deformation,[4,11–21] but a few studies have let open the possibility that this is not the case for lipids near protein inclusions and looked into it,[22,23] although not in the way we do here. Since the volume strain $u_V = \Delta V/V$ can be expressed, to lowest order, as the sum of the area strain $u_A = \Delta A/A$ and the thickness strain $u_D = \Delta D/D$, one has

$$u_V = u_A + u_D. \tag{1}$$

Incompressibility (*i. e.*, $\Delta V = 0$) enforces the ratio of u_A to u_D to be -1, which then implies a Poisson ratio of $\nu = \frac{1}{2}$.

Any sizable deviation from the constant volume assumption could, of course, have consequences for biophysical studies that in one way or another rely on a membrane's elastic properties. For instance, a lipid volume change would also occur in membranes containing mechanosensitive channels and could affect their gating when they are activated by a mechanical surface tension.[15,16,18,19] The passive permeability of such membranes would also increase due to both thinning of the membrane and lower mass density, but not necessarily by the same amount due to the two effects.[24]

Experimentally, it is difficult to obtain the Poisson ratio by directly measuring both ΔA and ΔD. The continuum mechanics relations developed in Section II show us how to obtain ν using other quantities from experiment and simulation, namely, the isothermal area compression modulus K_A already mentioned, and the isothermal bulk modulus K_V along with the membrane thickness D. However, there is also ambiguity in the parameters that occur in the continuum mechanics model. Fortunately, simulations obtain data that remove this ambiguity. The data are reviewed in Section III along with results for ν.

This continuum mechanics approach assumes that bilayers are homogeneous. However, lipid membranes exhibit structure that rapidly varies in the transverse z-direction. We know of no experimental data that can test whether this heterogeneity effects a conceivably *depth-dependent* Poisson ratio $\nu(z)$; but, as is often the case, simulations can address properties not accessible to experiment. In Section IV we therefore define $\nu(z)$ and

[a)] Current address: LPTMS, CNRS, Univ. Paris-Sud, Université Paris-Saclay, 91405 Orsay, France
[b)] E-mail: deserno@andrew.cmu.edu
[c)] E-mail: nagle@cmu.edu

determine it from a refined analysis of the same set of simulations.

II. RELATIONS FOR THE POISSON RATIO ν FOR A FLUID MEMBRANE

The harmonic free energy density f of an elastic body can generally be written as

$$f = \frac{1}{2}\lambda_{ijkl}u_{ij}u_{kl} \ , \tag{2}$$

where u_{ij} is the strain tensor and repeated indices are summed over the three spatial dimensions. After exploiting a membrane's in-plane translational and rotational symmetry, as well as its fluidity, this reduces to[25–27]

$$f = \frac{1}{2}\lambda_A u_A^2 + \frac{1}{2}\lambda_z u_z^2 + \lambda_{Az}u_A u_z \ , \tag{3}$$

where the notation has been simplified by introducing $\lambda_A = \lambda_{xxxx} = \lambda_{yyyy}$, $\lambda_z = \lambda_{zzzz}$, $\lambda_{Az} = \lambda_{xxzz}$, $u_A = u_{xx} + u_{yy}$ and $u_z = u_{zz}$. It has previously been assumed that $\lambda_A = \lambda_z$, because it simplifies some calculations.[25] In this paper we instead allow for an *elastic asymmetry*

$$\alpha := \frac{\lambda_z - \lambda_A}{\lambda_A} \ , \tag{4}$$

whose value we then estimate.

Eqn. (3) neglects a term that accounts for lipid tilt; but such a deformation involves non-diagonal strains, like u_{xz}, that appear not to be of concern for Poisson ratio considerations. Likewise, the elastic free energy of lipid membranes also contains a term proportional to a transbilayer lateral pre-stress, $\sigma_0(z)$;[11] but since the zeroth moment of this pre-stress vanishes, and none of our deformations are z-dependent, it also drops out of all subsequent considerations.

To obtain the Poisson ratio ν in terms of the elastic moduli entering Eqn. (3), one fixes a value of u_z and determines the ensuing u_A that minimizes f,

$$0 = \left(\frac{\partial f}{\partial u_A}\right)_{u_z} = \lambda_A u_A + \lambda_{Az}u_z \ , \tag{5}$$

which gives

$$\nu := -\frac{u_A}{2u_z} = \frac{\lambda_{Az}}{2\lambda_A} \ . \tag{6}$$

It proves convenient to re-express Eqn. (3) in terms of the Poisson ratio ν and the elastic asymmetry α; two equivalent forms, which differ in the choice of independent strains, will be used:

$$\frac{f(u_A,u_z)}{\lambda_A} = \frac{1}{2}u_A^2 + \frac{1}{2}(1+\alpha)u_z^2 + 2\nu u_z u_A \ , \tag{7a}$$

$$\frac{f(u_A,u_V)}{\lambda_A} = \frac{1}{2}u_V^2 + \frac{\alpha}{2}(u_V - u_A)^2 + (2\nu - 1)u_A(u_V - u_A) \ . \tag{7b}$$

Next we obtain expressions for the experimentally determined moduli. The area modulus K_A is defined by

$$\min_{u_z}\left\{Df(u_A,u_z)\right\} = \frac{1}{2}K_A u_A^2 \ , \tag{8}$$

where D is the thickness of the membrane.

Enforcing the minimization condition via Eqn. (7a) leads to

$$(1+\alpha)\,u_z + 2\nu\,u_A = 0 \ . \tag{9}$$

Solving this equation for u_z, inserting its value into Eqn. (7a), and combining with Eqn. (8), we find

$$\frac{K_A}{D\lambda_A} = \frac{1+\alpha-4\nu^2}{1+\alpha} \ . \tag{10}$$

Similarly, the experimentally determined bulk modulus K_V is defined by

$$\min_{u_A}\left\{f(u_A,u_V)\right\} = \frac{1}{2}K_V u_V^2 \ . \tag{11}$$

Enforcing the minimization condition, this time via Eqn. (7b), leads to

$$(1+\alpha-4\nu)\,u_A - (1+\alpha-2\nu)\,u_V = 0 \ . \tag{12}$$

Solving this equation for u_A, reinserting into Eqn. (7b), and combining with Eqn. (11), we find

$$\frac{K_V}{\lambda_A} = \frac{(1+\alpha)-4\nu^2}{\alpha+2(1-2\nu)} \ . \tag{13}$$

For subsequent analysis of experimental and simulation data, it is convenient to consider the ratio between a membrane's area- and bulk modulus. Dividing Eqn. (10) by Eqn. (13) eliminates the less convenient modulus λ_A and gives

$$\rho := \frac{K_A}{DK_V} = \frac{2(1-2\nu)+\alpha}{1+\alpha}. \tag{14}$$

Notice the occurrence of the membrane thickness D, which arises for dimensional reasons.

Rearranging Eqn. (14), we can also expresses the Poisson ratio ν in terms of two in principle measurable elastic modulus ratios, ρ and α:

$$\nu = \frac{1}{2} - \frac{\rho}{4} + \alpha\frac{1-\rho}{4} \ . \tag{15}$$

In passing, it is interesting to note that Eqn. (14) allows ν to be larger than $\frac{1}{2}$ for small ρ when α is positive. Although this may seem surprising in view of the well-known limit that indeed holds for isotropic elastics, it should be appreciated that there are no bounds on ν in the much larger universe of anisotropic elastic materials.[28] However, our system is constrained to $|2\nu| \leq 1+\alpha$ in order to satisfy the stability requirement

that both K_A and K_V be non-negative in Eqns. (10) and (13).

We finally obtain the relative volume change u_V resulting from a given area strain u_A. Setting $(\partial f/\partial u_V)_{u_A} = 0$ in Eqn. (7b) leads us to the associated *strain ratio* s,

$$s := \frac{u_V}{u_A} = \frac{1+\alpha-2\nu}{1+\alpha} \ . \tag{16}$$

In the next section we will determine values for the two ratios ρ and s, from which we then proceed to calculate the observables of interest: Poisson ratio ν and elastic asymmetry α. It is hence convenient to express the latter set directly in terms of the former:

$$\nu = \frac{1-s}{2(1+\rho-2s)} \ , \tag{17a}$$

$$\alpha = \frac{2s-\rho}{1+\rho-2s} \ , \tag{17b}$$

III. DATA AND RESULTS FOR HOMOGENEOUS FLUID MEMBRANES

The definition of the modulus ratio ρ in Eqn. (14) involves the area expansion modulus K_A, the bulk modulus K_V, and the membrane thickness D. Experimental work has established that K_A depends remarkably weakly on the specific lipid under study; it typically has a value around $(250 \pm 50)\,\mathrm{mN/m}$.[1,14,29,30] This range of values is encompassed in the first column of Table I for the four experimental rows.

Because isotropic pressure P and its conjugate thermodynamic variable V are relatively less interesting than the more relevant canonical surface pressure π and surface area A pair, fewer experimental results exist for a lipid bilayer's bulk modulus $K_V = -V(\partial P/\partial V)_T$ than for its area modulus $K_A = -A(\partial\pi/\partial A)_T$. However, the value 1.3 GPa has been measured for K_V for DPPC (1,2-dipalmitoyl-*sn*-glycero-3-phosphocholine) bilayers in the fluid phase at $T = 47.4°\mathrm{C}$.[31] A somewhat larger value of 2.2 GPa has been reported for the shorter chain length lipid DMPC (1,2-dimyristoyl-*sn*-glycero-3-phosphocholine) in its fluid phase at lower temperatures near $T = 30°\mathrm{C}$.[32] Although another study of DPPC under pressure did not quote a value for K_V,[33] from their Fig. 1 we estimate $K_V = 0.9\,\mathrm{GPa}$ in the fluid phase of DPPC at $T = 45.13°\mathrm{C}$ and a smaller value of $K_V \sim 0.6\,\mathrm{GPa}$ closer to the main transition $T_\mathrm{M} = 41.4°\mathrm{C}$. It is well known that there is anomalous softening of the bending modulus K_C in the fluid phase as the main transition is approached[34,35] and an even more pronounced softening has recently been reported for the tilt modulus K_θ.[36] The few data for K_V suggest a similar but weaker trend. A non-lipid bilayer (and non-anomalous) comparison is n-hexadecane, for which K_V is about 0.6 GPa at $T = 45°\mathrm{C}$.[37] Although hexadecane has similar hydrocarbon chains as DPPC, it is an isotropic liquid with more gauche-trans disorder than DPPC,[38] so its bulk modulus would be expected to be smaller. On the other hand, nearly 30% of the volume of lipids is in the headgroup region, which, being surrounded by water, is not likely to be compressible beyond that of the water. This would not change ΔV, but it would reduce the effective compressible volume V factor in K_V, thereby reducing its relevant value by 30%, closer to that of hexadecane. Based on all these considerations, we will consider the range of experimental estimates for K_V shown in Table I.

The D dependence in ρ, necessitated by dimensionality, causes some conceptual difficulties, because membrane thickness is microscopic, and how to define a geometric reference surface within a molecular-scale object is neither obvious nor in practice unique.[12] Two frequently encountered reference surfaces in the context of membrane bending are a leaflet's pivotal plane,[39] at which bending leads to no area strain, or its neutral surface,[40] at which bending and stretching energies decouple. However, these surfaces are introduced to conceptually localize strain or simplify elastic energies, not to serve as definitions of bilayer thickness—and hence they are not usually used for this purpose. A more common way to specify a membrane's transverse dimension is the Luzzati thickness D_B, which refers to the surface that arises when one imagines expelling all water from the headgroup region and rearranging the lipids to form a *gedanken* sheet of pure lipid. This definition approaches the problem thermodynamically, in the spirit of a Gibbs dividing surface. Typically, D_B has values around 3.6 nm.[41] An alternative structure-based definition is the hydrocarbon thickness, sometimes denoted $2D_\mathrm{C}$. It refers to the dividing surface for the methylene groups on the lipid tails. This choice identifies a bilayer with its hydrophobic lipid tail region; its value is about 2.7 nm for typical bilayers.[12] In our subsequent analysis we will examine both the Luzzati- and the hydrocarbon thickness, since they have different points in their favour. The Luzzati definition bridges between continuum theory and molecular reality without having to make a potentially arbitrary structural choice. The hydrocarbon thickness makes such a choice, but it is not arbitrary: simulations have shown that headgroup volume remains essentially constant with area strain,[42] consistent with it being immersed in water, and so one might not expect it to support anything other than $\nu = \frac{1}{2}$. Hence, the hydrocarbon thickness focuses on that part of the bilayer for which we would expect a "nontrivial" Poisson ratio.

Turning to simulations, row Sim 1 in Table I shows results from the only simulation[43] we could find that reported results for K_A and D, as well as data from which K_V can be extracted as we now show. What was reported using the CHARMM27r force field was a bulk modulus for the entire system of $K_\mathrm{sys} = (1.5 \pm 0.3)\,\mathrm{GPa}$. As nearly half ($\phi = 0.42$) of the system consisted of water, its contribution to the overall modulus must be taken out in order to arrive at the bulk modulus of the bilayer alone. Deviating slightly from the procedure proposed in Ref. [43], we note that the volume strains of the water-

and membrane-phase must add, which implies (in analogy to a springs-in-series argument)

$$\frac{1-\phi}{K_V} \;=\; \frac{1}{K_{\rm sys}} - \frac{\phi}{K_{\rm water}} \;. \tag{18}$$

Taking the value $K_{\rm water} = 2\,{\rm GPa}$ for the bulk modulus of TIP3P water from another CHARMM27r simulation,[44] we then find $K_V = 1.3\,{\rm GPa}$ for the bilayer in very good agreement with experiment.

Let us now turn to the strain ratio s. We are not aware of any experimental measurements of this variable, but we have been able to extract s from the simulation data (and later simulation trajectories) of Braun *et al.*,[42] who used the united atom force field GROMOS 43A1-S3[45] to simulate flat bilayers (288 DOPC (1,2-dioleoyl-*sn*-glycero-3-phosphocholine) lipids, 9428 SPCE water molecules) at $T = 29.85°{\rm C}$ under fixed (projected) area A. Of the several areas simulated we have picked five, equally spaced from $0.64\,{\rm nm}^2$ to $0.72\,{\rm nm}^2$, whose surface tensions γ had also been determined. The volumes of the total lipid, V_L, as well as of the hydrocarbon region alone, V_C, were obtained using a simple procedure[46] incorporated in the SIMtoEXP analysis software,[47] and values were reported in the Supplementary Material of Braun *et al.*.[42] As the simulation conditions are identical to those for Eqn. (16), we obtained the value of s from a plot of $\ln V$ versus $\ln A$. Using the entire lipid volume V_L corresponds to choosing the Luzzati thickness $D_{\rm B}$ as the membrane thickness; it gives $\partial(\ln V)/\partial(\ln A) = s = 0.0297 \pm 0.0041$. Using only the hydrocarbon volume corresponds to choosing the hydrocarbon thickness; it gives $s = 0.0399 \pm 0.0055$. The area modulus K_A and the thicknesses were also reported;[42] their values are shown in the Sim 2a and Sim 2b rows of Table I.

Table I illustrates ranges for the values of the K_A, K_V, and D data discussed in this section, and these give the values in the column of the modulus ratio ρ. For the D column, the smaller values are the hydrocarbon thicknesses and the larger values are the Luzzati thicknesses. The values in the s column come from the previous paragraph, and they correspond to the choice of D. The Poisson ratio is close to $\frac{1}{2}$, so Table I shows the difference $\frac{1}{2} - \nu$. That difference is largest for Case Exp 3 which puts K_A at its upper range and K_V at it lower range, and the difference even becomes slightly negative for the opposite end of the K_A and K_V ranges as seen for Case Exp 2. Using hydrocarbon thickness versus Luzzati thickness makes less difference as seen by comparing Cases Exp 1a and 1b and between Sim 2a and 2b; that is due to a compensating effect of s. Based on these four cases we suggest that $(\frac{1}{2} - \nu) \approx 0.015$, a 3% deviation from the usual assumption that $\nu = \frac{1}{2}$. The strain ratio s directly gives the relative volume change u_V for a given area strain u_A. Lipid bilayers typically rupture when the area strain u_A exceeds 6%,[48] so relative changes in volume would be less than 0.2% for Cases Exp 1a and 1b and Sim 2a and 2b.

Case	K_A [mN/m]	K_V [GPa]	D [nm]	ρ [10^{-2}]	s [10^{-2}]	$\frac{1}{2}-\nu$ [10^{-2}]	α [10^{-2}]
Exp 1a	250	1.3	3.6	5.3	3.0	1.2	0.7
Exp 1b	250	1.3	2.7	7.1	4.0	1.6	0.9
Exp 2	200	2.0	3.6	2.8	3.0	-0.1	3.3
Exp 3	300	0.6	3.6	14.	3.0	5.0	-7.3
Sim 1	138	1.3	3.9	2.7	3.0	0	3.4
Sim 2a	277	1.3	3.8	5.6	3.0	1.3	0.4
Sim 2b	277	1.3	2.8	7.6	4.0	1.8	0.4

TABLE I. Values of area modulus K_A, bulk modulus K_V, membrane thickness D, modulus ratio ρ from Eqn. (14), strain ratio s from Eqn. (16), deviation of the Poisson ratio ν from its usually assumed limit of $\frac{1}{2}$ from Eqn. (17a), and the elastic asymmetry α from Eqn. (17b), for a select set of cases discussed in the text.

The final column in Table I provides, to the best of our knowledge, the first estimate for the magnitude of the elastic asymmetry α from Eqn. (4), which quantifies the extent to which the diagonal elements $\lambda_A = \lambda_{xxxx} = \lambda_{yyyy}$ and $\lambda_z = \lambda_{zzzz}$ of the general elastic from Eqn. (3) differ from one another because a membrane's anisotropy breaks full rotational symmetry. The values for Cases Exp 1a and 1b and Sim 2a and 2b suggest that λ_z is about 0.5% larger than λ_A. However, uncertainties in the ratios ρ and s are consistent with $\alpha = 0$, so we simply conclude that any symmetry breaking is quite small.

It may also be noted that a coarse-grained simulation study obtained elastic ratios,[49] but it does not appear to relate those results to the classical Poisson ratio defined in Section II.

IV. INHOMOGENEOUS POISSON RATIO

A fluid lipid bilayer is laterally uniform, but along the normal direction it exhibits significant inhomogeneity, for instance in terms of its structure,[12] or lateral pressure profile,[11,50,51] or even its lateral area modulus profile.[27] This need not imply that results using homogeneous elasticity theory are wrong; but it behooves us to examine this issue, especially since any sizable variation with position could have implications for other theories which instead assume that ν is uniform (and close to $\frac{1}{2}$). It is furthermore of interest whether it is possible to operationally ascribe a *local Poisson ratio* to characteristize subregions of the bilayer.

A first and relatively straightforward step in this direction is to recognize the elastic difference between a membrane's head group region compared to the hydrocarbon tails. As noted above, a detailed analysis of molecular volumes indeed indicates that lipid head group moieties essentially do not change their volume upon bilayer stretching.[42] If so, the volume change is confined to the

hydrocarbon tails, and so we expect the bilayer-averaged value of $\frac{1}{2}-\nu$ to be larger when the focus is only on the hydrocarbon region as shown in Table I by the cases Exp 1a and 1b and by Sim 2a and Sim 2b.

Let us now strive to go beyond a binary division between heads and tails and define a truly *local* Poisson ratio $\nu(z)$. As we know of no experiment that has the sensitivity to measure inhomogeneity in the Poisson ratio at such a small scale, we once more turn to simulation and propose a refined way to analyze the previous set of simulations.[42]

At first glance, it might seem promising to examine how much the mean positions $z_{\rm m}$ of various molecular groups 'm' move as the membrane strain varies. Such an approach would be flawed, though, because the overall distribution of material varies as the molecular conformations perforce vary. This is especially easy to understand with regard to the terminal methyl groups, because a surprisingly larger fraction of the chain ends turn back towards the headgroup region when chain packing becomes more jumbled at larger area per lipid.[52,53] Indeed, the simulations[42] readily show that the proportion of terminal methyls in a central slab of thickness 1 nm decreases when the membrane area A is increased.

Our way to address this issue is by taking the focus away from individual lipids, or specific locations within them, and instead consider the total amount of material, no matter of what provenance, within specified regions of space. Consider therefore material slabs of thickness $2L(M)$ centered on the bilayer midplane, where the argument M identifies how much material is contained within the slab. If we now consider different areas A_i, the constraint of fixed M then yields the associated values of L_i. In the simulations different areas A_i were enforced by imposing a biaxial strain, and hence the condition required by Eqn. (9) which gives:

$$-\frac{2\nu_{12}(M)}{1-\delta} = \frac{u_D}{u_A} = \frac{\Delta L(M)}{\langle L(M)\rangle}\Big/\frac{\Delta A}{\langle A\rangle} \tag{19a}$$

$$= \frac{L_1(M)-L_2(M)}{L_1(M)+L_2(M)}\Big/\frac{A_1-A_2}{A_1+A_2}\,. \tag{19b}$$

To implement Eqn. (19b), we must define how much material is in a slab. Consider for instance the hydrocarbon region. Even though it is dominated by methylene groups, there are also terminal methyls and the methine groups at the double bonds in DOPC. We assume that all of these additively contribute to M, but in different proportions and with different weights. For the Poisson ratio, which focuses on volumes, the appropriate weight for each component is its volume. As already mentioned, component volumes have been previously reported for each simulated area.[42] Since differences in the *ratios* of the component volumes, shown in Table S1 of that paper, have little area dependence, we used the same weights for all areas—relative to a weight of unity for methylenes: $w_{\rm CH_3}=1.969$, $w_{\rm CH_1}=0.890$, $w_{\rm PO_4}=1.229$, $w_{2(\rm COO)}=2.899$, $w_{\rm Gly}=2.425$, $w_{\rm Chol}=5.683$ and $w_{\rm water}=1.118$.

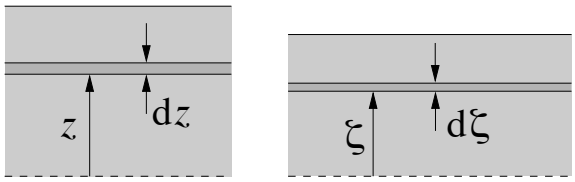

FIG. 1. Geometry and coordinates in a stress-free and a laterally stressed piece of flat material.

We emphasize that we only fix the relative weights; fixing the component volumes would perforce require $\nu=\frac{1}{2}$.

Instead of just calculating Poisson ratios for central slabs, let us proceed now to a method that allows using simulations at many areas to obtain a Poisson ratio as a function of z. Therefore, we can read our defining equation in a *localized version*,

$$-\frac{u_D(z)}{u_A} = \frac{2\nu(z)}{1+\alpha}, \tag{20}$$

where $\nu(z)$ is the depth-dependent value of the Poisson ratio, and where the z-coordinate must be defined via a "material perspective" analogous to the one outlined above.

To be more specific, consider one of the simulated areas, A_z, to be a reference area and focus on a thin slice $\mathrm{d}z$ within the bilayer. For a different simulated area, A_ζ, we can write the local z-strain as

$$u_D(z) = \frac{\mathrm{d}\zeta-\mathrm{d}z}{(\mathrm{d}\zeta+\mathrm{d}z)/2} = -2\,\frac{1-\mathrm{d}\zeta/\mathrm{d}z}{1+\mathrm{d}\zeta/\mathrm{d}z}\,, \tag{21}$$

where ζ is the height-variable corresponding to the stretched bilayer, in the manner described after Eqn. (19b) (see also Fig. 1). Using Eqn. (20) to eliminate $u_D(z)$ yields

$$\frac{\nu(M)}{1+\alpha} = \frac{1}{u_A}\times\frac{1-\mathrm{d}\zeta/\mathrm{d}z}{1+\mathrm{d}\zeta/\mathrm{d}z} \tag{22}$$

for each area strain u_A.

We used simulation data for five different bilayer systems featuring areas per lipid of $(64,66,68,70,72)\,\text{Å}^2$, choosing $68\,\text{Å}^2$ as the reference A_z, and directly calculated the area strains for the other four areas as

$$u_A = \frac{A_\zeta-A_z}{(A_\zeta+A_z)/2}\,. \tag{23}$$

Using the same relative volume weights for the component groups of lipids (terminal methyls, methylenes, methines, etc.) as above, we determine a set of $\zeta(z)$ values that corresponds to the same amount of material in the central slab between $\zeta(z)$ and $-\zeta(z)$ (for each area). We numerically differentiated $\zeta(z)$ for each area strain u_A to obtain $\mathrm{d}\zeta/\mathrm{d}z$, which together with Eqn. (22) yields four estimates of $\nu(z)/(1+\alpha)$ from which we obtain averages with stadard deviations for the uncertainties. It may be

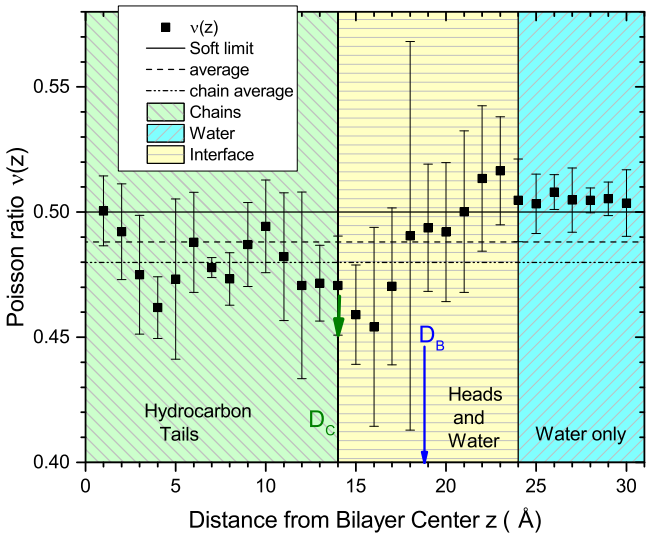

FIG. 2. Position-dependent Poisson ratio $\nu(z)$ as a function of distance z from the bilayer midplane, obtained from an atomistically simulated DOPC bilayer.[42] The first average is over all z and the second average is only for the chain region. Overlaid are the simulated main structural regions with the hydrocarbon thickness D_{C} and the Luzzati thickness D_{B} indicated by arrows.

noted that the elastic asymmetry α could conceivably depend upon z, but we know of no way to investigate that. Rather, given the small value of α suggested by Table I and the errors of our local strains, we will proceed by ignoring α altogether.

Our main result for the z-dependent Poisson ratio is shown in Figure 2. In the region in which there is only water, $z \gtrsim 2.3\,\mathrm{nm}$, $\nu(z)$ is statistically consistent with a value of $\frac{1}{2}$. For smaller z, the respective averages of $\nu(z)$ are consistent with the value obtained from the homogeneous analysis in Section II. More precisely, averaging $\nu(z)$ over the hydrocarbon region yields $\frac{1}{2} - \langle\nu(z)\rangle_{\mathrm{hc}} = 2.1\times10^{-2}$, quite close to the Sim 2b value, in which we proposed a Poisson ratio within the hydrocarbon region using simpler arguments. Looking beyond averages, there appear to be two small "dips" that are borderline statistically significant: one at $z \approx 0.4\,\mathrm{nm}$, and one at $z \approx 1.6\,\mathrm{nm}$ (near the location of the glycerol groups). We explored whether these oscillations could be removed by varying the relative weights of the component groups. Although this affected the values of $\nu(z)$ somewhat, we found no set of weights that eliminated the small oscillations.

V. DISCUSSION

Our observations, derived from both experiment and simulation, and summarized in Tab. I and Fig. 2, indicate that the Poisson ratio for lipid bilayers is close to $\frac{1}{2}$, with relative deviations about 3%. The predicted relative volume changes $\Delta V/V$ are very small, even for strains that would rupture most bilayers.[48] Therefore, we should be on safe ground when making the usual approximation that volumes do not change significantly under anisotropic mechanical stresses of biophysical interest.

The values of ν obtained by comparing experimental and simulation results (Cases Exp 1a compared to Sim 2a and EXP 1b compared to Sim 2b), and the values determined in our simulation (Cases Sim 2a and 2b) are in remarkably good agreement. This is to some extent fortuitous, though, since the experimental values for K_V and K_A have neither been determined for the same lipid, nor at the same temperature. Likewise, values of K_A, K_V and s have not been obtained from the same simulation. It would be valuable to do simulations on the same system, varying both lateral pressure and bulk pressure, to obtain the three quantities independently.

While the most immediate lesson of our work is confirmation that a lipid bilayer is nearly perfect soft matter, in the sense that it is highly deformable relative to its bulk compressibility, there may be more to be learned from further considering the local Poisson ratio. Admittedly, the variations in $\nu(z)$, as extracted from our data, are statistically not very compelling; but they would be highly interesting if true and might merit following up on. Observe that the deviation in $\frac{1}{2} - \nu$ at $z = 1.6\,\mathrm{nm}$ in Fig. 2 is about three times as large as in regions away from the two "dips." This means that $K_A(z)/K_V(z)$ is about three times larger, or, relatively speaking, it is about three times harder to stretch membranes at this particular depth than elsewhere. This is intriguing, because the location where area strain is found to be particularly expensive happens to coincide with the location of the pivotal plane, where area strain indeed vanishes. Moreover, Fig. 2 also suggests that the "active region" for deviations of $\nu(z)$ from $\frac{1}{2}$ is not limited to the hydrocarbon region, but appears to extend into the headgroup region nearly as far as the Luzzati thickness D_{B}.

Our z-dependent findings are consistent with observations by Campelo *et al.*,[27] who have shown (on the basis of simulations using the MARTINI[54,55] model) that the lateral stretching modulus profile has indeed a maximum near the neutral surface (which is not identical to, but quite close to,[56] the pivotal plane). To determine this profile, they followed an entirely different technique, based on monitoring the tension-dependence of the lateral pressure profile. This, however, requires measuring stresses fairly precisely, which is computationally expensive. In contrast, our method for accessing $K_A(z)/K_V(z)$ via the Poisson ratio relies exclusively on keeping track of local bilayer material rearrangements, which can be done based on configurations alone, without calculating stresses or energies. It is hence conceptually easier and can—potentially—be done with higher accuracy. The idea is similar in spirit to a recent proposal to measure the ratio of tilt and bending modulus by counting the

fraction of lipids within slices of buckled membranes—*i. e.*, again by a *purely geometric* procedure.[57]

VI. CONCLUSION

In this paper we have shown that lipid bilayers behave like typical soft condensed matter, having a Poisson ratio that deviates about 3% from the common soft matter limit of $\nu = \frac{1}{2}$. While not unexpected, this fills a niche in the elasticity theory of membranes, and it supports the approximation used in many theories that area and thickness deformation are strongly coupled, with only a negligible correction due to volume change. We have also seen that the elastic asymmetry α describing the difference between the lateral and perpendicular diagonal elements of the full elastic tensor deviate by less than 1%.

Beyond this homogeneous finding, any depth dependence of the Poisson ratio, or of a membrane's elastic moduli, would surely have profound implications for a number of local membrane processes, such as protein insertion, gating of channels (especially mechanosensitive ones), fission, and fusion. This simply mirrors some of the interesting possibilities opened by the depth dependence of the lateral pressure profile. However, it seems safe to expect in the foreseeable future that the study of locally resolved constitutive relations must rely on simulation approaches, for lack of sufficient resolution in present experimental techniques. This paper is a step in that direction.

ACKNOWLEDGMENTS

JFN acknowledges Fred Sachs for conversations about the theory of mechanosensitive channels that led him to this study. We acknowledge Alex Sodt for pointing out that we had originally not properly taken into account in-plane fluidity. MD acknowledges funding from the National Science Foundation via grant CHE 1764257.

[1]Rawicz W, Olbrich KC, McIntosh TJ, Needham D, Evans E. Effect of chain length and unsaturation on elasticity of lipid bilayers. Biophys J. 2000;79(1):328–339.

[2]Pan J, Tristram-Nagle S, Nagle JF. Effect of cholesterol on structural and mechnaical properties of membranes depends on lipid chain saturation. Phys Rev E. 2009;80(2):021931(1–12).

[3]Deserno M. Fluid lipid membranes: From differential geometry to curvature stresses. Chem Phys Lipids. 2015;185:11–45.

[4]Doktorova M, V LM, Khelashvili G, Weinstein H. A new computational method for membrane compressibility: Bilayer mechanical thickness revisited. Biophys J. 2019;116.

[5]Nagle JF. Area Compressibility Moduli of the Monolayer Leaflets of Asymmetric Bilayers from Simulations. Biophys J. 2019;117:1051–1056.

[6]Templer RH, Khoo BJ, Seddon JM. Gaussian curvature modulus of an amphiphilic monolayer. Langmuir. 1998;14(26):7427–7434.

[7]Siegel DP, Kozlov MM. The Gaussian curvature elastic modulus of N-monomethylated dioleoylphosphatidylethanolamine: relevance to membrane fusion and lipid phase behavior. Biophys J. 2004;87(1):366–374.

[8]Siegel DP. The Gaussian curvature elastic energy of intermediates in membrane fusion. Biophys J. 2008;95(11):5200–5215.

[9]Hu M, Briguglio JJ, Deserno M. Determining the Gaussian curvature modulus of lipid membranes in simulations. Biophys J. 2012;102(6):1403–1410.

[10]Hu M, de Jong DH, Marrink SJ, Deserno M. Gaussian curvature elasticity determined from global shape transformations and local stress distributions: a comparative study using the MARTINI model. Faraday Discuss. 2013;161:365–382.

[11]Hamm M, Kozlov MM. Elastic energy of tilt and bending of fluid membranes. Eur Phys J E. 2000;3(4):323–335.

[12]Nagle JF, Tristram-Nagle S. Structure of lipid bilayers. Biochim et Biophys Acta Rev Biomembranes. 2000;1469(3):159–195.

[13]Nielsen C, Andersen OS. Inclusion-induced bilayer deformations: Effects of monolayer equilibrium curvature. Biophys J. 2000;79:2583–2604.

[14]Henriksen JR, Ipsen JH. Measurement of membrane elasticity by micro-pipette aspiration. Eur Phys J E. 2004;14:149–167.

[15]Wiggins P, Phillips R. Analytic models for mechanotransduction: gating a mechanosensitive channel. Proc Nat Acad Sci (USA). 2004;101(12):4071–4076.

[16]Wiggins P, Phillips R. Membrane-protein interactions in mechanosensitive channels. Biophys J. 2005;88(2):880–902.

[17]Pan D, Wang W, Liu W, Yang L, Huang HW. Chain packing in the inverted hexagonal phase of phospholipids: a study by x-ray anomalous diffraction on bromine-labeled chains. J Am Chem Soc. 2006;128(11):3800–3807.

[18]Reeves D, Ursell T, Sens P, Kondev J, Phillips R. Membrane mechanics as a probe of ion-channel gating mechanisms. Phys Rev E. 2008;78(4):041901.

[19]Sachs F, Sivaselvan MV. Cell volume control in three dimensions: Water movement without solute movement. J Gen Physiology. 2015;145(5):373–380.

[20]Nagao M, Kelley EG, Ashkar R, Bradbury R, Butler PD. Probing elastic and viscous properties of phospholipid bilayers using neutron spin echo spectroscopy. J Phys Chem Letts. 2017;8:4679–4684.

[21]Terzi MM, Deserno M. Novel tilt-curvature coupling in lipid membranes. J Chem Phys. 2017;147(8):084702.

[22]Brannigan G, Brown FLH. Contributions of Gaussian Curvature and Nonconstant Lipid Volume to Protein Deformation of Lipid Bilayers. Biophys J. 2007;92:864–876.

[23]Sodt AJ, Beaven AH, Andersen OS, Im W, Pastor RW. Gramicidin A Channel Formation Induces Local Lipid Redistribution II: A 3D Continuum Elastic Model. Biophys J. 2017;112:1198–1213.

[24]Mathai JC, Tristram-Nagle S, Nagle JF, Zeidel ML. Structural determinants of water permeability through the lipid membrane. J Gen Physiology. 2008;131(1):69–76.

[25]Kozlov MM, Leikin SL, Markin VS. Elastic properties of interfaces. Faraday Trans 2. 1989;85:277–292.

[26]Campelo F, McMahon HT, Kozlov MM. The hydrophobic insertion mechanism of membrane curvature generation by proteins. Biophys J. 2008;95:2235–2339.

[27]Campelo F, Arnarez C, Marrink SJ, Kozlov MM. Helfrich model of membrane bending: From Gibbs theory of liquid interfaces to membranes as thick anisotropic elastic layers. Adv Colloid Interface Sci. 2014;208:25–33.

[28]Ting TCT, Chen TY. Poisson's ratio for anisotropic elastic materials can have no bounds. J Mech Appl Math. 2005;58:73–82.

[29]Rawicz W, Smith BA, McIntosh TJ, Simon SA, Evans E. Elasticity, strength, and water permeability of bilayers that contain raft microdomain-forming lipids. Biophys J. 2008;94(12):4725–4736.

[30]Evans E, Rawicz W, Smith BA. Concluding remarks back to the future: mechanics and thermodynamics of lipid biomembranes. Faraday Disc. 2013;161:591–611.

[31]Tosh RE, Collings P. High pressure volumetric measurements in dipalmitoylphosphatidylcholine bilayers. Biochim Biophys Acta. 1986;859:10–14.

[32]Vennemann N, Lechner MD, Henkel T, Knoll W. Densitometric Characterization of the Main Phase Transition of Dimyristoyl-Phosphatidylcholine between 0.1 and 40 MPa. Ber Bunsenges Phys Chem. 1986;90(10):888–891.
[33]Liu NI, Kay RL. Redetermination of the pressure dependence of the lipid bilayer phase transition. Biochem. 1977;16(15):3484–3486.
[34]Lemmich J, Mortensen K, Ipsen JH, Honger T, Bauer R, Mouritsen OG. Small-angle neutron scattering from multilamellar lipid bilayers: Theory, model, and experiment. Phys Rev E. 1996;53:5169–5180.
[35]Chu N, Kučerka N, Liu Y, Tristram-Nagle S, Nagle JF. Anomalous swelling of lipid bilayer stacks is caused by softening of the bending modulus. Phys Rev E. 2005;71(4):041904.
[36]Nagle JF. X-ray scattering reveals molecular tilt is an order parameter for the main phase transition in a model biomembrane. Phys Rev E. 2017 SEP 12;96(3).
[37]Weast RC. CRC Handbook of Chemistry and Physics. 60th ed. CRC Press; 1980.
[38]Nagle JF, Wilkinson DA. Lecithin bilayers. Density measurement and molecular interactions. Biophys J. 1978;23(2):159–175.
[39]Rand RP, Fuller NL, Gruner SM, Parsegian VA. Membrane curvature, lipid segregation, and structural transitions for phospholipids under dual-solvent stress. Biochem. 1990;29(1):76–87.
[40]Kozlov MM, Winterhalter M. Elastic moduli for strongly curved monoplayers. Position of the neutral surface. J Phys II (France). 1991;1(9):1077–1084.
[41]Kučerka N, Tristram-Nagle S, Nagle JF. Structure of fully hydrated fluid phase lipid bilayers with monounsaturated chains. J Mem Biol. 2006;208(3):193–202.
[42]Braun AR, Sachs JN, Nagle JF. Comparing simulations of lipid bilayers to scattering data: the GROMOS 43A1-S3 force field. J Phys Chem B. 2013;117(17):5065–5072.
[43]Venable RM, Skibinsky A, Pastor RW. Constant surface tension molecular dynamics simulations of lipid bilayers with trehalose. Mol Sim. 2006;32(10-11):849–855.
[44]Venable RM, Chen LE, Pastor RW. Comparison of the extended isotropic periodic sum and particle mesh Ewald methods for simulations of lipid bilayers and monolayers. J Phys Chem B. 2009;113:5855–5862.
[45]Chiu SW, Pandit SA, Scott H, Jakobsson E. An improved united atom force field for simulation of mixed lipid bilayers. J Phys Chem B. 2009;113(9):2748–2763.
[46]Petrache HI, Feller SE, Nagle JF. Determination of component volumes of lipid bilayers from simulations. Biophys J. 1997;72(5):2237–2242.
[47]Kučerka N, Katsaras J, Nagle JF. Comparing membrane simulations to scattering experiments: introducing the SIMtoEXP software. J Membr Biol. 2010;235(1):43–50.
[48]Olbrich KC, Rawicz W, Needham D, Evans E. Water Permeability and Mechanical Strength of Polyunsaturated Lipid Bilayers. Biophys J. 2000;79(1):312–327.
[49]Jadidi T, Seyyed-Allaei H, Rahimi Tabar MR, Mashaghi A. Poisson's ratio and Young's modulus of lipid bilayers in different phases. Front Bioeng Biotechnol. 2014;2:1–6.
[50]Rowlinson JS, Widom B. Molecular theory of capillarity. Mineola, NY: Dover; 2002.
[51]Cantor RS. The lateral pressure profile in membranes: a physical mechanism of general anesthesia. Biochem. 1997;36(9):2339–2344.
[52]Xu ZC, Cafiso DS. Phospholipid packing and conformation in small vesicles revealed by two-dimensional 1H nuclear magnetic resonance cross-relaxation spectroscopy. Biophys J. 1986;49(3):779–783.
[53]Feller SE, Yin D, Pastor RW, MacKerell Jr AD. Molecular dynamics simulation of unsaturated lipid bilayers at low hydration: parameterization and comparison with diffraction studies. Biophys J. 1997;73(5):2269–2279.
[54]Marrink SJ, Risselada HJ, Yefimov S, Tieleman DP, De Vries AH. The MARTINI force field: coarse grained model for biomolecular simulations. J Phys Chem B. 2007;111(27):7812–7824.
[55]Marrink SJ, Tieleman DP. Perspective on the Martini model. Chem Soc Rev. 2013;42(16):6801–6822.
[56]Leikin S, Kozlov MM, Fuller NL, Rand RP. Measured effects of diacylglycerol on structural and elastic properties of phospholipid membranes. Biophys J. 1996;71(5):2623–2632.
[57]Wang X, Deserno M. Determining the lipid tilt modulus by simulating membrane buckles. J Phys Chem B. 2016;120(26):6061–6073.